NJC

New Journal of Chemistry

A journal for new directions in chemistry

Accepted Manuscript

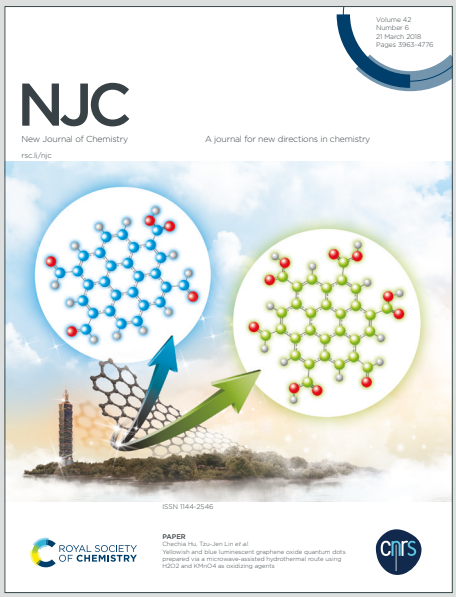

View Article Online
DOI: 10.1039/C9NJ02234A

ARTICLE

The study of *cis–trans* isomerization preference of *N*–alkylated peptides containing phosphorus in the side chain and backbone.

Received 00th January 20xx,
Accepted 00th January 20xx

DOI: 10.1039/x0xx00000x

Alexander F. de la Torre, *[a] Akbar Ali, [b] Odette Concepcion, [a] Ana L. Montero-Alejo, [c] Francisco M. Muñiz, [a] Claudio A. Jiménez, [a] Julio Belmar, [a] José Luis Velázquez–Libera, [d] Erix W. Hernández–Rodríguez, *[e] and Julio Caballero [d]

The current work provides a study on the *cis–trans* isomerization behaviour of *N*–alkylated peptides decorated with phosphonate ester group. Ugi four–component reaction was chosen for the synthesis of *N*–alkylated peptides, where almost only the *cis* isomer was detected when the phosphonate ester group was incorporated as amine component in the side chain. However, the phosphonate ester group inserted in the backbone, as an isocyanide component, leads preferably to the *trans* isomer of this kind of peptides. The diverse behaviour of *cis–trans* isomerization has been explained via spectroscopic nuclear magnetic resonance analysis and computational calculations.

Introduction

Phosphopeptides are the class of pseudopeptides in which at least an amide linkage or *C*–terminal carboxyl group has been replaced by a phosphoryl, phosphonate ester or phosphonamide functional group. [1] In nature, this class of compounds represents a versatile group of chemical scaffolds with many biological applications. [1,2] In this context, it is worth mentioning that phosphonate moieties inserted in several chemical structures are associated with strong antimicrobial, [1,3] antiparasitic [4] and antiviral activities. [5] Today, the crisis of "bacterial resistance to the antibiotics" is a concern for the pharmaceutical industries and public health sectors around the globe. One possible solution to this end is to introduce foldamers to the drug market as a non–biocidal class of compounds to eradicate bacterial resistance. [6,7] Thus, foldamers might be the best choice against diseases that are not possible to treat with small organic molecules. *N*–alkylated peptides or 'peptoids' are a class of foldamers constructed to mimic properties of peptides. [8,9] Solution– and solid–phase peptide synthesis are the most recently used techniques to obtain *N*–alkylated peptides in an adequate way. [10] Importantly, a well–established amino acid sequence may be used to insert the desired side chain in *N*–alkylated peptides structures that could be employed for conformational investigations. However, the major challenge is to control the *cis*/*trans* conformation yield at the tertiary amide bond of *N*–alkylated peptides.

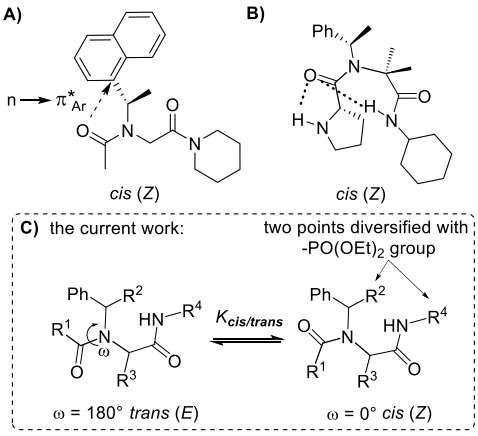

Figure 1. *Cis–trans* amide isomerism (A and B) driven by intramolecular n→π* or/and hydrogen interactions occurring in *N*–alkylated peptides. [12, 14] C) The current work.

In this scenario, various studies have been focused on the *cis–trans* amide isomerism, principally on peptoids carrying the main backbone structure like *N*–alkylglycine peptide, [11] where intramolecular n→π* interactions contribute considerably to the conformational distribution. Notwithstanding, n→π* interactions between the carbonyl oxygen of amides and the electron–deficient aromatic group is crucial to induce the controlled production of *cis* over *trans* isomer. [12] Besides, the *α*–chiral amide side chains also can lead to the conformational *cis–trans* equilibrium of *N*–alkylated peptides (Figure 1A). [12a] Hydrogen bond (HB) also plays a pivotal role in the *cis–trans* isomerization. In this aspect, *N*–hydroxy amide or hydroxamic acid in the side chain of *N*–alkylated peptide has a preference for *cis* (*Z*) instead of *trans* (*E*) isomer. [13] Also, *N*–substituted amino acid Aib structures shows preference for *cis* conformation, driven by an intramolecular HB as can be seen in Figure 1B. [14]

[a] Departamento de Química Orgánica, Facultad de Ciencias Químicas, Universidad de Concepción, Concepción, Chile. afernandezd@udec.cl
[b] Department of Chemistry, University of Sargodha, 40100, Pakistan.
[c] Departamento de Física, FCNMM, Universidad Tecnológica Metropolitana, José Pedro Alessandri 1242, Ñuñoa, 780-0002, Santiago, Chile; & Núcleo Milenio MULTIMAT, Chile.
[d] Centro de Bioinformática y Simulación Molecular (CBSM), Universidad de Talca, 1 Poniente No. 1141, Casilla 721, Talca, Chile.
[e] Escuela de Química y Farmacia. Facultad de Medicina. Universidad Católica del Maule, 3460000 Talca, Chile. ehernandez@ucm.cl
† Footnotes relating to the title and/or authors should appear here.
Electronic Supplementary Information (ESI) available: [details of any supplementary information available should be included here]. See DOI: 10.1039/x0xx00000x

View Article Online
DOI: 10.1039/C9NJ02074A

Despite the numerous available reports on the structural analysis of *N*–alkylated derivates, none describes the three–dimensional structural adaptation of phosphopeptides. Therefore, the conformational study of peptoids containing phosphorus is of valuable academical, industrial and commercial interest due to their potentialities to develop novel therapeutic drugs. Thus, herein we present a study of the cis/trans behaviour of synthesized *N*–alkylated peptides containing phosphorus as shown in Figure 1C.

Results and discussion

Isocyanide–based multicomponent reactions (IMCR) are efficient protocols to assemble *N*–alkylated peptides in a single operation either in solution or even in the solid phase approach.[15] A few reports have been referred to obtain *N*–alkylated peptides containing phosphorus moiety by multicomponent reactions – e.g. Ugi and Orru reactions –. [16] Thus, our group, on the ongoing study of the rational design and synthesis of new potential LasB inhibitor ligand with an embedded phosphorus moiety through Ugi four–component reaction (Ugi–4CR), we decided to investigate the amide bond isomerization of the *N*–alkylated peptide obtained. To be more precise, we restricted our study to the *N*–substituted amino acid Gly compounds particularly where phosphonate ester group (POEG) was incorporated either as an amine in the side chain or isocyanide component in the backbone of the peptoids. Besides, paraformaldehyde was mostly used as the oxo component (R^3 = H) in the Ugi–4CR (see Scheme 1 and Scheme 2). However, aromatic and aliphatic aldehyde were also introduced (e.g. compounds 7 and 8, Scheme 1). Compounds 3 to 8 were obtained with the commercially available amine diethyl (*α*–aminobenzyl) phosphonate as racemic form.

Consequently, we have synthesized a library of seventeen *N*–alkylated peptides with phosphorus atom linked by using Ugi–4CR; which induced a high molecular diversity by employing different amino acids (AA), dipeptides and lipidic analogues (Scheme 1 and Scheme 2). Initially, compounds 1, 2 and 3 have been individually chosen in order to match the substitution effect (R^2) in the side chain. These compounds were achieved in high to moderate yields (89%, 78%, and 52%, respectively) by processing in a one–pot manner where the acetic acid, paraformaldehyde, cyclohexyl isocyanide, and different amines have been employed to explore the influence of the side chain over the *cis–trans* amide isomerization (Scheme 1). In compounds 1, 2, and 3, R^2 substituent moieties correspond to *α*–H, (*S*)–*α*–Me and *α*–$PO(OEt)_2$ functions, respectively (Scheme 1). The *cis–trans* proportion was determined by the NMR (1D) study in $CDCl_3$ (Figure 2). The *cis/trans* ratio of compounds 1 and 2 was in agreement with similar *N*–alkylated peptides previously reported in 2013.[14] By comparing, the assigned ^{1}H NMR spectra of compounds 1, 2 and 3, it is easy to identify that compound 3 shows a preference towards a single isomer (Figure 2). Compounds 1 and 2 shows two broad signals corresponding to the *N*H group (labelled as A, see Figure 2), while compound 3 only shows one. These signals occur between 5 and 7 ppm, and the deshielded signals should correspond to the isomer that involves the strongest non–covalent intramolecular interaction with the *N*H group. It is also expected that the CH groups that support R^2 substitutions interact with both, the carbonyl and methyl of the acetyl groups, and consequently two signals of the CH groups should appear whether both isomers are present. These are the cases of compounds 1 and 2 with the signals (labelled as B in Figure 2) at 4.66/4.62 and 6.16/5.13 ppm, respectively.

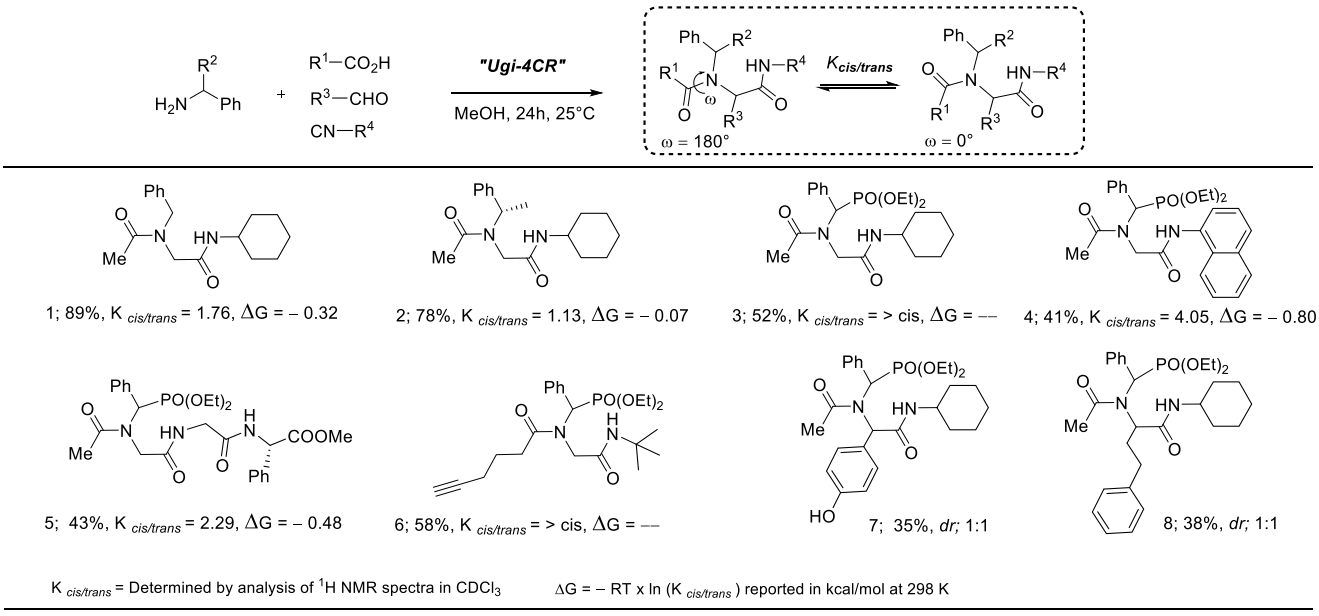

Scheme 1. *N*–alkylated peptides model system structures 1–6 synthesized by Ugi–4CR.
Cis/trans ratios ($K_{cis/trans}$) and corresponding free energy differences (ΔG).

View Article Online
DOI: 10.1039/C9NJ02354A

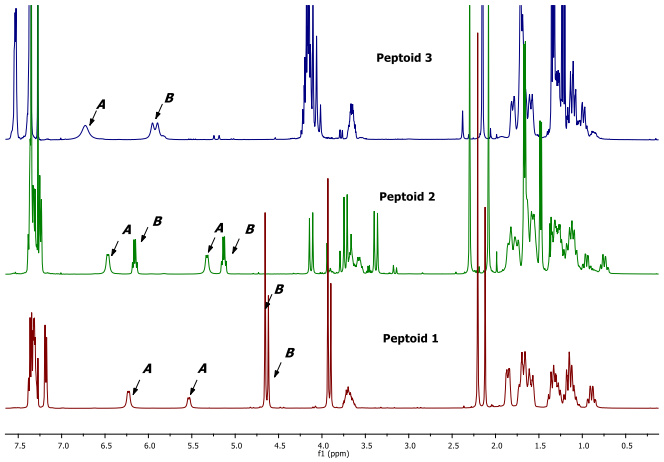

Figure 2. 400 MHz ^{1}H NMR spectra in $CDCl_3$ of compounds 1 (redline), 2 (greenline) and 3 (blueline). (A) correspond to *N*H of secondary amide and (B) correspond to protons of CH groups that support R^2 substitutions.

In contrast, the CH group linked to POEG in compound 3 shows a single doublet signal at 5.92 ppm. The high chemical shift corresponds to the strong intramolecular interaction with the carbonyl group in the *cis* isomers. The complete assignment of the ^{1}H and ^{13}C NMR spectra, and the bidimensional COSY, HSQC and HMBC spectra of peptoid 3 explain that it should preferably be in *cis* conformation (Supporting information, part A). Consequently, the NOESY spectrum shows a cross peak between the protons of methyl of the acetyl group and the methylene group of the backbone peptidic skeleton (Xaa = Gly) at 2.14 and 4.10–4.05 ppm, respectively. In addition, there is no cross–peak of NOE between the signals at 5.92 ppm of CH attached to POEG and methyl of the acetyl group (2.14 ppm), which prevents the assignment of the *trans* conformation of this compound.

We also introduce different substituent by changing the isocyanide component in the Ugi–4CR. Subsequently, compounds 4 and 5 were obtained maintaining the effect of the PO(OEt)2 group in the side chain as in compound 3. NMR analysis shows a high *cis/trans* ratio suggesting that stability is governed by intramolecular interactions similar to those of compound 3. However, the considerable ability to form intramolecular interactions of the R^4 anchor groups in 4 and 5, could explain some stabilization of the *trans* conformers. Additionally, we investigated the conformational behaviour of compound 6 by using different acidic and isocyanide components (e.g. hexynoic acid and *tert*–butyl isocyanide). Again, a preference for the cis isomer was detected for this compound, which shows that neither a long chain as an acid component nor bulkiest substituent affect the population of the adopted isomer (Scheme 1). We also recorded ^{1}H–NMR spectra in four different deuterated solvents (see Supporting Information, Part A) in order to verify the interaction strengths that provide this stereoselectivity. The polarity of the solvent did not affect the cis conformation, suggesting that this *N*–alkylated peptide variant is stabilized by strong intramolecular interactions, as was interpreted above. In order to evaluate the effect of the oxo component R^3 in the *cis–trans* isomerization of peptoids, 4–hydroxybenzaldehyde and hydrocinnamaldehyde were employed instead of paraformaldehyde (compounds 7 and 8, Scheme 1). As we can observe in the ^{1}H and ^{13}C NMR spectra in Supporting Information (part A), for both compounds, a diastereomeric ratio of 1:1 was obtained. Unfortunately, this poor diastereoselectivity does not allow us to clearly evaluate the effect of R^3 on the *cis/trans* isomerization.

The POEG was also incorporated into the backbone of the *N*–alkylated peptide skeleton for the study of *cis–trans* equilibrium. Diethylisocyanomethyl phosphonate was also utilized in the Ugi–4CR protocol (Scheme 2). Both compounds 9 and 11 are the structural references of the peptoids 1 and 2, excepting the changes on the isocyanide component. The combination of ^{1}H, ^{13}C, DEPT–135°, COSY, HSQC, and HMBC spectra allowed to perform the assignment of all carbon and proton of 9 as well as to reveal the preference of *trans* conformer over the *cis* one, i.e., in a 3:1 *trans/cis* ratio (See Supporting Information, Part A). The protons of *N*H group, methylene of the peptide backbone and methyl of the acetyl groups, are each distributed in two signals corresponding to the presence of both isomers. Through the NOESY spectrum, a NOE was detected between the methylene protons associated with the side chain at 4.65 ppm and the methyl of the acetyl group at 2.20 ppm, assigned to the *trans* isomer. To verify the intramolecular interaction strengths that provide the ratio of isomers obtained, we measured the ^{1}H–NMR spectrum of compound 9 in four different deuterated solvents ($CDCl_3$, DMSO–d_6, D_2O, and CD_3OD). Table 1 shows the corresponding $K_{cis/trans}$ values. Notice that, unlike the experience with peptide 6, here the *trans/cis* ratio is significantly affected while the polarity of the solvent increases. This result suggests a weaker intramolecular HB than that observed for compounds 3 and 6. According to the structure, a seven–member ring formed by a HB between the *N*H group with the carbonyl of the acetyl groups (–NH····O=C–) (see Table 1), could explain this sensitive stabilization of the trans conformer.

The phosphonic acid group in the *N*–alkylated peptide backbone lead to a slight drop in the $K_{cis/trans}$ value (0.44 for compound 10, Scheme 2). The insertion of the phosphonic acid group (compound 10) increases the *trans*/*cis* amide conformer ratio because the acidic OH groups can establish a HB with the amide moiety, and compete with the HB between acetyl and amide moiety (–C=O····HN–) as shown in Table 1.

Subsequently, we introduce a chiral substituent in the side chain (R^2 = (*S*)–*α*–Me) identifying that this steric hindrance has no effects in the isomer ratio, having similar $K_{cis/trans}$ values for both compounds 9 and 11. Similarly, a lipidic amino acid, as the acid component inserted in the synthesized *N*–alkylated peptide, [14,15b] induces predominantly a *trans* conformation of 12 (see Scheme 2). Importantly, when the *N*–protected AA Boc–Pro was employed as the acid component (compound 13) instead of acetic acid, the *cis/trans* ratio was affected. Moreover, the integrated aminoisobutyric (Aib) structures (compound 14) by using propanone as the oxo component of *N*–alkylated peptide showed a more favourable *cis* conformation with respect to *N*–alkylglicine (compound 13).

View Article Online
DOI: 10.1039/C9NJ02374A

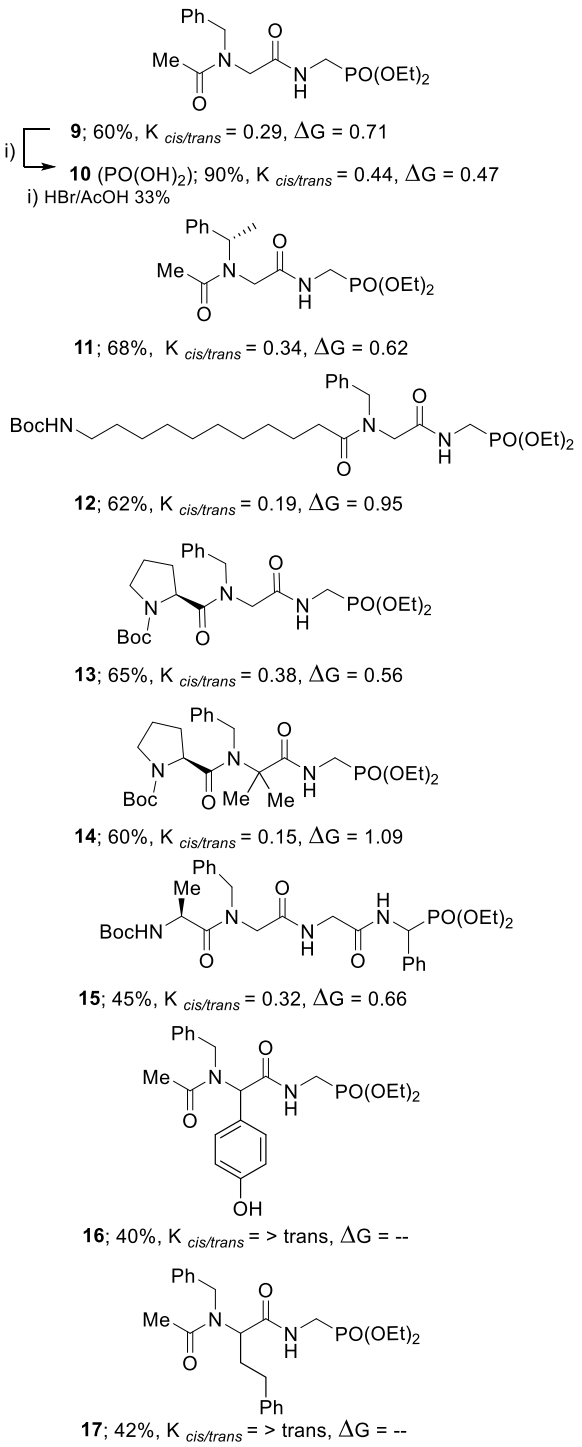

Scheme 2. Peptoids structures 9–17 with the *cis/trans* ratios ($K_{cis/trans}$) and their free energy differences (ΔG).

The adopted structure by this type of backbone remains over a beta–turn motif that is more favourable for the *trans* conformation in the *N*–alkylated peptide. Thus, a unique rotamer of Aib compound 14 has been identified by the NMR analysis. The chain elongation of pseudopeptides usually causes destabilization of the *trans* conformation as other intramolecular interactions such as HB and could lead to an increase in the *cis* population by decreasing the energetic barrier of *cis*–*trans* isomerization. We also introduced POEG as the isocyanide dipeptide (i.e., CN–Gly–Phg–$PO(OEt)_2$) for the preparation of *N*–alkylated tetrapeptide 15 (Scheme 2). [17] Interestingly, even when the aforementioned *trans* conformation should be more favourable for compound 15 however, the NMR analysis reveals the contrary, only the *cis* rotamer was observed.

Table 1. $K_{cis/trans}$ ratios for compound 9 in various deuterated solvents and their free energies differences (*ΔG*) expressed in kcal/mol. The structural representation of compound 9.

Solvent	$K_{cis/trans}$[a]	ΔG[b]
$CDCl_3$	0.29	0.71
DMSO–d_6	0.67	0.23
D_2O	0.67	0.23
CD_3OD	0.75	0.17

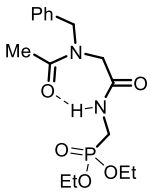

a) Determined by ^{1}H NMR spectroscopy analysis of 15 mM compound solutions at 25°C. b) $\Delta G_{cis/trans} = -$ RT x ln ($K_{cis/trans}$) reported in kcal/mol.

Under the same idea explored in compounds 7 and 8, we also introduced the oxo component 4–hydroxybenzaldehyde and hydrocinnamaldehyde into the skeleton of peptoids, but in this case, the phosphorus atom is placed at the backbone of the skeleton (compounds 16 and 17, Scheme 2). In the ^{1}H and ^{13}C NMR spectra of both compounds, solely the trans conformer were observed (see Supporting Information, Part A). This behaviour can be explained for the n→π*$_{Ar}$ interaction [12] between the carbonyl oxygen of the acetyl group and the aromatic group employed as oxo component (R^3) and do not by HB as previously discussed. In order to assess which isomer was obtained, we used compound 16 for further NMR spectroscopic characterization (See Supporting Information, Part A). The NOESY and ROESY experiments permits to ensure the preference of *trans* conformer over *cis*. A NOE between the protons of methyl related to the acetyl group at 2.06 ppm and the protons of methylene associated with the benzyl group at 4.65 ppm and 4.52 ppm has been detected. Also, a NOE between the *α*–CH of 16 in the backbone at 5.77 ppm and the protons of methyl at 2.06 ppm was observed. Besides, a NOE between the methyl of the acetyl group at 2.06 ppm and the protons of the aromatic ring in R^3 also show that the preferred isomer is the *trans*.

Computational analysis

A conformational analysis using the OPLS–2005 force–field [18] and a GB/SA chloroform solvent model [19] was performed to achieve a better understanding of the *cis*/*trans* preference of the synthesized *N*–alkylated peptides 3 and 9 by using Monte Carlo multiple–minimum (MCMM) method as implemented in Macromodel version 9.9. [20] Thus, we were able to identify 228 conformers for each enantiomer (*S*)–3 or (*R*)–3 clustered in 11 and 15 groups, respectively; as well as 333 conformers clustered in 28 groups corresponding to the compound 9 (see Supporting Information, Part B) with energy within 5 kcal/mol. The low

energy structures of each group were recalculated at the quantum mechanics (QM) level (M06–2X/6–31G(d)// M06–2X/6–31+G(d, p)) considering the universal solvation model based on the density (SMD) to simulate the effect of chloroform. This procedure leads to verify the quality of the MCMM method in the conformational search since the type of isomer or the number of non–redundant conformers practically did not change while using QM. There were only two conformations of 9 converging with each other. From the refined energies, electronic and Gibbs free, the analysis of Boltzmann populations at 25 ˚C shows that the representative populations of these models of *N*–alkylated peptide in solution are in agreement with the NMR analysis. Compound 3, either *S* or *R* enantiomer, preferentially adopts cis conformations (over 99 % Boltzmann populations), while the models of compound 9 appears like a mixture of isomers of *cis/trans* conformations (27:73 % Boltzmann populations), see Figures S1–S3; Tables S1–S5 in the Supporting Information Part B.

Figure 3 shows the superpositions of the lower energy structures obtained (optimized QM) from (*S*)–3 and 9. These representations illustrate the conformational rigidity of 3 with respect to 9. On the right side of the overlay, the geometry of the lowest energy conformer shows the typical intramolecular interactions observed in each case (green dotted lines, Figure 3).

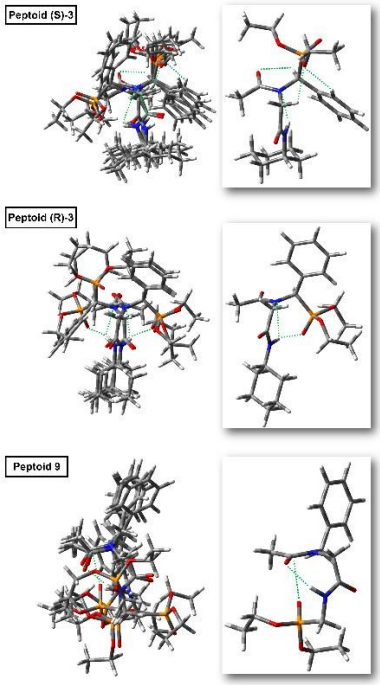

Figure 3. Overlay of the representative (lower–energy) structures of the compounds (*S*)–3 (top), (R)–3 (medium), and 9 (bottom) reoptimized at the M06–2X/6–31+G(d,p)//M06–2X/6–31+G(d) theory level with implicit chloroform as the solvent.

Notice that, according to the NMR predictions, strong intramolecular interactions prevail in all representations of compound 3 (Figure 3). One between the CH groups that support the R^2 substitution with the carbonyl of the acetyl group, and the other between the NH group and the nitrogen atom of the tertiary amide, that forms a stable five–membered ring; that kind of hydrogen bond (NH····N) has been well described in peptidic structures. [21,22] On the other hand, compound 9 is mainly represented by a structure stabilized by a seven–membered ring formed by a HB between the NH group and the carbonyl of the acetyl groups (–NH····O=C–), which is very sensitive to the polarity of the solvent according to the NMR analysis. In addition, there are important interactions involving the POEG in the analysed peptides that will be analysed below.

The positive (+) and negative (–) orientations of the dihedrals φ (C=N–C_α–C) and ψ (N–C_α–C=N) have also assigned in each conformer (Tables S4 and S5, Supporting Information –Part B). A unique *cis* isomer was calculated for the compound (*S*)–3 exhibiting a *cis*/*trans* isomer ratio of 100:0, this isomer form is distributed among the +/+ and –/– orientations of ψ/φ angles (Table 2). Similarly, the *cis* isomer of the compound (*R*)–3 appears as the more energetically favourable conformation showing a more accentuated tendency to the +/+ dihedral orientation. Most of the minority *cis* isomers identified for compound 9 show the dihedral ψ/φ orientations +/+ and –/– whereas the *trans* conformations were almost totally distributed between orientations +/– and –/+.

Table 2. Isomers and dihedral distributions for peptoids (*S*)–3, (*R*)–3, and 9, according to the sum of the corresponding Boltzmann populations.

Peptoid	Isomer	$\psi(+)/\varphi(-)$	$\psi(-)/\varphi(+)$	$\psi(+)/\varphi(+)$	$\psi(-)/\varphi(-)$
(S)–3	***cis***	0,00	21,28*	52,30	26,34
	trans	0,00	0,08**	0,00	0,00
(R)–3	***cis***	4,62	10,1	78,27	6,94
	trans	0,00	0,08	0,00	0,00
9	***cis***	0,00	2,71	5,20	19,24
	trans	14,56	57,08	0,00	1,21

*Sum of the Boltzmann population corresponding to the *cis* conformation of the global minimum, obtained from the most populated *cis* (starting conformation) after performing Intrinsic Reaction Coordinate (IRC) calculations; **sum of the Boltzmann population corresponding to the final *trans* conformation obtained after performing IRC calculations to simulate the *cis*–*trans* isomerization of (*S*)–3.

From the lowest–energy conformations of the stereoisomer (*S*)–3 and peptoid 9, we evaluated the energetic cost of the isomerization by modelling the transition state (TS). We start to consider the conformer 8 of (*S*)–3, which represent the largest percentage of the population (25 %) in its *cis* configuration (8–*cis*). This conformation evolves to a close rotamer (rot–8–*cis*) from which the TS yields a *trans* conformation with an activation energy of 21 kcal/mol, using the same level of theory as the QM optimization, see Figure 4 (top). The weighted values of Gibbs free energies and Boltzmann populations, as well as the ψ/φ dihedral distributions were also calculated for the rot–8–*cis* (12–*cis*) and 13–*trans* rotamers. These intermediate conformers were obtained along the reaction path between the lowest–energy *cis* and final *trans* isomers of compound (*S*)–3, as shown in Figure 4 (top), and highlighted in the Supporting Information, Part B. While, the molecular–mechanics starting structures used to obtain the quantum mechanics optimized conformers from 1 to 11, coming from MCMM simulations (Supporting Information, Part B). Neither rot–8–*cis* nor the *trans* conformation has been obtained as representative

structures of conformational sampling. Nonetheless, they were added as conformers 12 and 13 respectively in Table S5 of the SI, to analyse their probability of occurrence according to the weighted energies. Notice that for 3, the *trans* conformer (13–*trans*) is significantly less stable than 8–*cis* and only represent 0.1 % of the population according to the Boltzmann distribution. This means that the equilibrium is shifted towards the less energetic *cis* isomers, which explains the configurational stiffness of this compound.

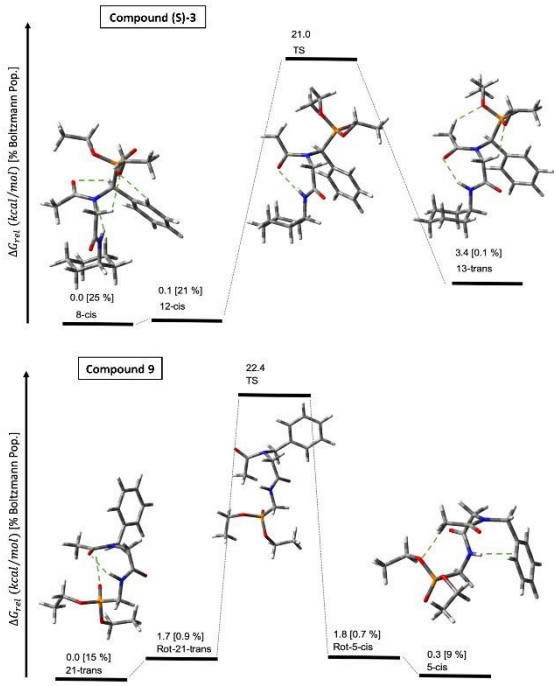

Figure 4. Gibbs free energy profile of the isomerization mechanism of (*S*)–3 (top) and 9 (bottom) at the M06–2X/6–31+G(d,p) // M06–2X/6–31+G(d) theory level with implicit chloroform as the solvent.

In contrast, the isomerization of the compound 9 models leads to stable products (ΔG_{rel} = 0.3 kcal/mol); both appear as representative at room temperature (15 % and 9 % for *trans* and *cis* Boltzmann population respectively), see Figure 3 (bottom). The activation energy, in this case, is practically the same as required to isomerize compound 3 from *cis* to *trans* and is in the range of those obtained for similar *N*–alkylated peptides but with different anchor groups. [14] In order to gain more insight into the interactions stabilizing *cis*/*trans* conformations, we used the natural bond orbital population analysis (NBO).

We considered the stabilization energy (delocalization energy) of the relevant intramolecular (spatial) interactions between the NBO orbitals (represented as dashed green lines in Figure 4 and quantitatively in Table S7 of the SI). In general, the analysis revealed that the HB interactions between the oxygen lone pair $LP_{C=O}$ of the tertiary amide carbonyl group and the NH group (i.e., amide group) of the contiguous peptoid bond ($LP_{C=O} \rightarrow \sigma^*_{H-N}$) seem to be necessary to stabilize the *trans* conformation for both compounds. Note that the delocalization energies of these interactions in the ground–state conformations are in the range from 5 to 7 kcal/mol. However, according to this analysis, this condition does not seem to be enough to stabilize the ground state. For instance, the lower energy structures of the (*S*)–3 peptoid are all *cis* configurations and do not show this interaction. The presence of other intramolecular interactions in a cooperative effect seems sufficient to explain the propensity to adopt the *cis* conformation. The lowest energy structure of the (*S*)–3 (8–*cis*), in addition to the stable five–membered ring explained by the interaction NH–N, shows a network of the relatively strong interactions (~2.5 kcal/mol) that includes the oxygen lone pairs, either of the carbonyl or the phosphonate ester group, with the CH groups of backbone, side chains and even phenyl group (see Figure 4 and Table S7). The representative *trans* isomer of the peptide 9 (21–*trans*) shows the strongest HB interactions ($LP_{C=O} \rightarrow \sigma^*_{H-N}$), but also a stabilizing n–π*interaction with the phosphonate group ($LP_{P=O} \rightarrow \pi^*_{C=O}$). The latest interaction does not appear in the representative 5–*cis* conformer. However, the 5–*cis* conformer is stabilized principally by the $LP_{P=O(OEt)2} \rightarrow \sigma^*_{H-C}$ (2.3 kcal/mol) and the NH—π interaction (1.75 kcal/mol). From the NBO analysis, the sum of these relatively weak interactions could explain the stability of the *cis* conformation of 9. In general, the influence of the phosphonate ester group is less significant when it is attached in the backbone. However, according to our analysis, the phosphonate ester group attached to the side chain mediates stabilizing interactions of the *cis* isomer. This is expected in some way since the presence of the phosphonate ester group at R^2 supports the steric control.

Experimental

Material and methods

Materials and reagents were of the highest commercially available grade and used without further purification. ^{1}H NMR and ^{13}C NMR spectra were recorded at 400 MHz for ^{1}H and 100 MHz for ^{13}C, respectively. Chemical shifts (δ) are reported in parts per million relative to the residual solvent signals, and coupling constants (J) are reported in hertz. High–resolution mass spectra (HRMS) were recorded using electron spray ionization (ESI) (Hybrid linear ion trap–orbitrap FT–MS and QqTOF/MS – Microtof – QII models).

General procedure for the Ugi–4CR

The *N*–alkylated peptides were prepared according to literature procedure.[15b] Dissolution of the amine (0.5 mmol, 1.0 equiv.), the aldehyde (or ketone) (0.5 mmol, 1.0 equiv.), the carboxylic acid (0.5 mmol, 1.0 equiv.) and the isocyanide (0.5 mmol, 1.0 equiv.) in MeOH (5 mL) were stirred at 25°C for 24 h.

Compound 1. Yield: 129 mg (89%) as colourless oil. A mixture of rotamers was observed by NMR (ratio 6:4). Assigned signals belong to the mixture of rotamers where (*) correspond to the major rotamer. R_f = 0.51 (hexane/EtOAc 1:1 v/v). ^{1}H NMR (400

View Article Online
DOI: 10.1039/C9NJ02274A

MHz, $CDCl_3$) δ 7.39 – 7.28 (m, 4H), 7.18 (d, J = 7.3 Hz, 1H), 6.23*, 5.53 (2×d, J = 6.8 Hz, 1H, NH), 4.66*, 4.62 (2×s, 2H), 3.93*, 3.90 (2×s, 1H), 3.75 – 3.62 (m, 1H), 2.21*, 2.12 (2×s, 3H), 1.91 – 1.82 (m, 1H), 1.76 – 1.54 (m, 4H), 1.41 – 1.04 (m, 5H), 0.89 (qd, J = 12.1, 2.9 Hz, 1H). ^{13}C NMR (100 MHz, $CDCl_3$) δ 172.05*, 171.66, 168.04*, 166.98, 137.10, 135.93*, 129.18, 129.11, 128.76, 128.18, 127.99, 126.71, 53.45*, 52.67, 50.83, 50.60*, 48.38, 48.24*, 32.95*, 32.85, 25.60*, 25.42, 24.86, 24.80*, 21.81, 21.56*. HRMS (ESI–FT–ICR) m/z: 311,1729 $[M+Na]^+$; calcd. for $C_{17}H_{24}N_2O_2Na$: 311,1735.

Compound 2. Yield: 118 mg (78%); as a colourless oil. A mixture of rotamers was observed by NMR (ratio 1:0.9). Assigned signals belong to the mixture of rotamers where (*) correspond to the major rotamer. R_f = 0.54 (hexane/EtOAc 1:1 v/v). ^{1}H NMR (400 MHz, $CDCl_3$) δ 7.34 (dq, J = 8.6, 7.0 Hz, 1H), 7.24 (d, J = 7.5 Hz, 1H), 6.47*, 5.32 (2×d, J = 6.7 Hz, 1H), 6.16*, 5.13 (2×q, J = 7.1 Hz, 1H), 5.13 (q, J = 6.9 Hz, 1H), 4.13 (d, J = 15.2 Hz, 1H), 3.73 (d, J = 14.6 Hz, 1H), 3.66 (t, J = 9.2 Hz, 1H), 3.62 – 3.54 (m, 1H), 3.38 (d, J = 15.3 Hz, 1H), 2.30*, 2.08 (2×s, 3H), 1.80 (m, 1H), 1.66*, 1.28 (2×d, J = 7.0 Hz, 3H), 1.65 – 1.53 (m, 1H), 1.40 – 1.06 (m, 1H), 0.95–0.80*, 0.80 – 0.68 (2×m, 1H). ^{13}C NMR (100 MHz, $CDCl_3$) δ 171.90, 169.11, 167.64, 140.31, 139.69, 129.19, 129.02, 128.81, 128.26, 128.06, 127.71, 127.16, 126.69, 57.11, 55.75, 50.97, 48.25, 47.99, 47.88, 47.54, 32.91, 32.75, 32.61, 25.64, 25.43, 24.80, 24.76, 22.33, 22.04, 18.44, 16.31. HRMS (ESI–FT–ICR) m/z: 303,2073 $[M+H]^+$; calcd. for $C_{18}H_{27}N_2O_2$ Exact Mass: 303,2071.

Compound 3. Yield: 110 mg (52%); as a colourless oil. R_f = 0.54 (hexane/EtOAc 1:1 v/v). ^{1}H NMR (400 MHz, $CDCl_3$) δ 7.57 – 7.51 (m, 2H), 7.41 – 7.34 (m, 3H), 6.72 (bs, 1H), 5.92 (d, J = 23.1 Hz, 1H), 4.21 – 4.11 (m, 4H), 4.10 – 4.05 (m, 2H), 3.69 – 3.61 (m, 1H), 2.14 (s, 3H), 1.84 – 1.55 (m, 7H), 1.33 (t, J = 7.1 Hz, 3H), 1.28 (m, 2H), 1.21 (t, J = 7.1 Hz, 3H), 1.17 – 1.06 (m, 2H), 1.00 (dt, J = 20.9, 6.4 Hz, 1H). ^{13}C NMR (100 MHz, $CDCl_3$) δ 172.13, 167.32, 133.49, 129.66, 129.58, 129.19, 128.89, 63.82, 63.75, 62.85, 62.78, 51.85, 48.59, 32.82, 32.69, 25.47, 25.00, 21.79, 16.56, 16.50, 16.39, 16.33. HRMS (ESI–FT–ICR) m/z: 447,2021 $[M+Na]^+$; calcd. for $C_{21}H_{33}N_2O_5PNa$ Exact Mass: 447,2025

Compound 4. Yield: 95 mg (41%); as a brown amorphous solid. R_f = 0.35 (hexane/EtOAc 1:1 v/v). A mixture of rotamers was observed by NMR (ratio 6:4). Assigned signals belong to the mixture of rotamers where (*) correspond to the major rotamer. ^{1}H NMR (400 MHz, $CDCl_3$) δ 9.13*, 8.67(2×s, 1H, NH), 7.92 – 7.60 (m, 8H), 7.56 – 7.32 (m, 10H), 6.36*, 5.32 (2×d, J = 23.1 Hz, 1H), 4.47 (d, J = 18.1 Hz, 1H), 4.32 (d, J = 18.0 Hz, 1H), 4.22 – 4.05 (m, 4H), 2.46, 2.31* (2×s, 3H), 1.37 (dd, J = 8.1, 4.2 Hz, 1H), 1.28 (t, J = J = 6.9 Hz, 3H), 1.17 (t, J = 6.9 Hz, 3H), 1.04 (dd, J = 14.6, 7.2 Hz, 1H). ^{13}C NMR (100 MHz, $CDCl_3$) δ 172.55*, 172.50, 167.63, 134.27*, 133.28, 133.24, 132.04, 129.95, 129.87, 129.41, 129.26, 129.06, 128.64, 128.55, 127.77, 126.42, 126.36, 126.14, 125.61, 121.48, 121.44, 63.83, 63.76*, 63.31, 63.23*, 51.94*, 22.23, 22.09*, 16.71, 16.67, 16.62, 16.57, 16.48*, 16.42*, 16.35*, 16.29*. HRMS (ESI–FT–ICR) m/z: 491,1702 $[M+Na]^+$; calcd. for $C_{25}H_{29}N_2O_5PNa$: 491,1712.

Compound 5. Yield: 128 mg (43%); as a white amorphous solid. R_f = 0.20 (hexane/EtOAc 1:1 v/v). A mixture of rotamers was observed by NMR (ratio 6:4). Assigned signals belong to the mixture of rotamers where (*) correspond to the major rotamer. ^{1}H NMR (400 MHz, $CDCl_3$) δ 7.83 (t, J = 5.8 Hz, 1H), 7.55 – 6.95 (m, 10H), 6.83 (d, J = 7.1 Hz, 1H), 6.11 (d, J = 23.8 Hz, 1H), 4.85 (m, 2H), 4.25 – 4.07 (m, 6H), 4.03 – 3.84 (m, 5H), 3.75 (s, 3H), 3.72 – 3.64 (m, 5H), 3.23 – 3.06 (m, 6H), 2.12*, 2.04 (2×s, 3H), 1.31 (m, 5H), 1.18 (t, J = 7.1 Hz, 3H) 1.12 (t, J = 7.1 Hz, 3H). ^{13}C NMR (101 MHz, $CDCl_3$) δ 172.20, 171.91, 171.18, 169.05, 168.53, 162.75, 162.17, 136.39, 136.23, 135.92, 135.23, 135.06, 133.37, 129.81, 129.33, 129.25, 128.98, 128.86, 128.65, 127.62, 127.24, 127.13, 63.67, 63.36, 62.86, 61.32, 59.85, 53.54, 53.32, 52.73, 52.40, 50.67, 45.19, 43.16, 37.77, 37.54, 21.80, 16.34. HRMS (ESI–FT–ICR) m/z: 542,2020 $[M]^+$; calcd. for $C_{27}H_{35}N_2O_8P$: 546,2131

Compound 6. Yield: 131 mg (58%); as a white amorphous solid. R_f = 0.45 (hexane/EtOAc 1:1 v/v). ^{1}H NMR (400 MHz, $CDCl_3$) δ 7.62 – 7.50 (m, 2H), 7.36 (m, 3H), 6.19 (d, J = 23.1 Hz, 1H), 6.06 (b.s, 1H, NH), 4.20 – 4.13 (m, 2H), 4.09 (m, 2H), 2.46 (qd, J = 16.4, 8.0 Hz, 2H), 2.29 (td, J = 6.8, 2.6 Hz, 2H), 1.96 – 1.87 (m, 3H), 1.34 (t, J = 7.1 Hz, 3H), 1.20 (t, J = 7.1 Hz, 3H), 1.17 (s, 9H). ^{13}C NMR (101 MHz, $CDCl_3$) δ 173.84, 167.41, 133.45, 130.02, 129.94, 129.29, 128.97, 83.54, 69.41, 63.58, 63.51, 62.96, 62.89, 51.40, 50.94, 31.80, 28.46, 23.88, 17.86, 16.59, 16.53, 16.38, 16.32. HRMS (ESI–FT–ICR) m/z: 473,2169 $[M+Na]^+$; calcd. for $C_{23}H_{35}N_2O_5PNa$ Exact Mass: 473,2181

Compound 7. Yield: 91 mg (35%); as a light yellow amorphous solid. A mixture of diastereoisomers was observed by NMR (ratio 1:1). R_f = 0.30 (hexane/EtOAc 1:3 v/v). ^{1}H NMR (400 MHz, $CDCl_3$) δ 7.64 – 7.41 (m, 3H), 7.35 (m, 7H), 7.16 – 6.95 (m, 3H), 6.85 (m, 3H), 6.75 – 6.58 (m, 3H), 6.42 (m, 2H), 5.67 – 5.45 (m, 2H), 4.29 – 3.79 (m, 10H), 3.67 (m, 1H), 3.45 (m, 1H), 2.30 (s, 3H), 2.04 (s, 3H), 1.84 – 1.29 (m, 10H), 1.23 (m, 12H). ^{13}C NMR (100 MHz, $CDCl_3$) δ 172.28, 169.73, 164.34, 160.49, 157.46, 157.41, 136.51, 136.44, 134.66, 132.35, 131.17, 130.45, 129.21, 129.12, 128.95, 128.66, 128.60, 128.47, 128.33, 128.29, 128.13, 127.92, 127.89, 127.81, 127.38, 124.35, 116.17, 115.99, 115.96, 74.18, 72.64, 67.67, 65.04, 64.97, 63.85, 63.78, 63.41, 63.34, 61.76, 61.68, 60.53, 49.67, 48.59, 32.94, 32.76, 32.59, 25.42, 25.34, 25.28, 24.95, 24.78, 22.46, 21.15, 18.45, 16.52, 16.46, 16.40, 16.36, 16.29, 16.23, 14.29, 14.22.

Compound 8. Yield: 101 mg (38%); as a colourless oil. A mixture of diastereoisomers was observed by NMR (ratio 1:1). R_f = 0.40 (hexane/EtOAc 1:3 v/v). 1H NMR (400 MHz, CDCl3) δ 7.48 – 7.02 (m, 20H), 6.72 (bs, 1H), 6.63 (bs, 1H), 4.24 (d, J = 17.2 Hz, 2H), 4.01 (t, J = 9.8Hz, 2H), 4.17 – 3.73 (m, 10H), 3.44 (m 1H), 2.87 – 2.62 (m, 2H), 2.18 (s, 3H), 2.01 (s, 3H), 1.95 – 1.41 (m, 7H), 1.30 – 1.21 (m, 10H), 1.18 – 1.04 (m, 10H). ^{13}C NMR (100 MHz, CDCl3) δ 171.67, 171.63, 168.91, 167.26, 141.90, 137.72, 137.69, 129.92, 129.48, 129.10, 128.82, 128.62, 128.55, 128.50, 128.44,

128.36, 128.07, 128.01, 127.94, 127.91, 127.87, 127.83, 127.80, 127.74, 127.71, 127.68, 127.65, 127.62, 127.59, 125.96, 63.82, 63.75, 62.94, 62.87, 62.80, 62.73, 62.27, 62.20, 54.86, 53.38, 49.52, 48.52, 34.61, 32.73, 32.59, 32.36, 30.90, 25.50, 25.35, 24.92, 24.81, 22.64, 22.19, 21.71, 16.51, 16.46, 16.39, 16.33, 16.27, 16.22.

Compound 9. Yield: 108 mg (60%); as a colourless oil. A mixture of rotamers was observed by NMR (ratio 6:4). Assigned signals belong to the mixture of rotamers where (*) correspond to the major rotamer. R_f = 0.40 (hexane/EtOAc 1:1 v/v). ^{1}H NMR (400 MHz, $CDCl_3$) δ 7.40 – 7.29 (m, 4H), 7.18 (d, J = 7.1 Hz, 1H), 6.77*,6.43 (2×t, J = 4.0 Hz, 1H, NH), 4.65 (s, 2H), 4.17 – 4.08 (m, 4H), 4.01*,3.92 (2xs, 2H), 3.68 (dd, J = 12.1, 6.0 Hz, 2H), 2.21*, 2.14 (2×s, 3H), 1.33 (t, J = 7.1 Hz, 6H). ^{13}C NMR (100 MHz, $CDCl_3$) δ 172.09*, 171.59, 169.01*, 168.30, 136.84, 135.83*, 129.10, 128.84, 128.45, 127.99, 127.81, 126.65, 62.77, 53.24*, 50.92, 49.80, 49.38*, 35.48, 33.92, 21.64, 21.40*, 16.49. DEPT 135° (100 MHz, $CDCl_3$) δ 129.08 (CH), 128.89(CH), 128.47 (CH), 127.98 (CH), 126.58 (CH), 62.69 (CH_2), 62.62 (CH_2), 53.19 (CH_2), 51.16 (CH_2), 49.85 (CH_2), 49.63 (CH_2), 35.46 (CH_2), 33.91 (CH_2), 21.34 (CH_3), 16.44 (CH_3), 16.38 (CH_3). HRMS (ESI–FT–ICR) m/z: 379,1395 $[M+Na]^+$; calcd. for $C_{16}H_{25}N_2O_5PNa$: 379,1399

Compound 10. Yield 25mg (90%); as light yellow amorphous solid. A mixture of rotamers was observed by NMR (ratio 6:4). Assigned signals belong to the mixture of rotamers where (*) correspond to the major rotamer. R_f = 0.35 (MeOH/EtOAc 1:9 v/v). ^{1}H NMR (400 MHz, DMSO–d6) δ 8.25*, 8.03 (2×t, J = 5.3 Hz, 1H, NH), 7.44 – 7.15 (m, 5H), 3.88 (d, J = 11.2 Hz, 2H), 3.45 – 3.32 (m, 2H), 2.05, 2.01* (2×s, 3H). ^{13}C NMR (101 MHz, DMSO–d6) δ 171.45*, 171.09, 168.47*, 168.42, 138.12*, 137.67, 129.20, 128.85, 128.21, 128.08, 127.79, 127.49, 127.20, 62.31, 62.25, 52.59, 50.56*, 49.21*, 48.04, 37.67, 37.59, 36.16, 36.08, 21.84*, 21.70, 16.73*, 16.67. HRMS (ESI–FT–ICR) m/z: 299,0802 $[M–H]^+$; calcd. for $C_{12}H_{17}N_2O_5P$ Exact Mass: 300,0875

Compound 11. Yield: 126 mg (68%); as a colourless oil. A mixture of rotamers was observed by NMR (ratio 6:4). Assigned signals belong to the mixture of rotamers where (*) correspond to the major rotamer. R_f = 0.50 (hexane/EtOAc 1:1 v/v). ^{1}H NMR (400 MHz, $CDCl_3$) δ 7.43 – 7.31 (m, 3H), 7.25 (d, J = 7.5 Hz, 2H), 6.90*, 5.93 (2×t, J = 4.0 Hz, 1H, NH), 6.16, 5.16* (2×q, J = 6.8 Hz, 1H), 4.26 (d, J = 15.4 Hz, 1H), 4.19 – 4.06 (m, 4H), 3.84 – 3.70 (m, 2H), 3.54 (ddd, J = 22.4, 13.9, 8.0 Hz, 1H), 3.40 (d, J = 15.4 Hz, 1H), 2.32*, 2.12 (2×s, 1H), 1.69*, 1.51 (2×d, J = 7.0 Hz, 1H), 1.42, 1.35* (2×t, J = 7.1 Hz, 6H). ^{13}C NMR (101 MHz, $CDCl_3$) δ 172.17, 169.96, 139.48, 129.11, 128.13, 126.61, 62.64, 57.26, 47.09, 35.66, 33.71, 22.37, 18.48, 16.56, 16.50. HRMS (ESI–FT–ICR) m/z: 371,1738$[M+H]^+$; calcd. for $C_{18}H_{27}N_2O_5P$: 370,1658

Compound 12. Yield: 180 mg (62%); as a colourless oil. A mixture of rotamers was observed by NMR (ratio 6:4). Assigned signals belong to the mixture of rotamers where (*) correspond to the major rotamer. R_f = 0.40 (hexane/EtOAc 3:1 v/v). ^{1}H NMR (400 MHz, CDCl3) δ 7.43 – 7.23 (m, 4H), 7.18 (d, J = 7.2 Hz, 1H), 6.83, 6.65 (2xs, 1H, NH), 4.66 (s, 2H), 4.14 (p, J = 7.2 Hz, 4H), 4.01 (s, 2H), 3.69 (dd, J = 12.0, 5.9 Hz, 2H), 3.11 (m, 2H), 2.43 (t, J = 7.0 Hz, 2H), 2.32 – 2.27 (m, 1H), 1.73 – 1.56 (m, 2H), 1.45 (s, 9H), 1.34 (t, J = 7.1 Hz, 6H), 1.28 (m, 14H). ^{13}C NMR (100 MHz, CDCl3) δ 174.71, 169.14, 156.12, 136.10, 129.11*, 128.87, 128.49, 127.96*, 126.66*, 62.77, 62.71*, 52.43*, 49.67, 40.74, 35.52, 33.96*, 33.32, 33.10*, 30.16, 29.57, 29.46*, 29.36, 28.55, 26.90, 25.24*, 25.02, 16.55*, 16.49. HRMS (ESI–FT–ICR) m/z: 598,3610 $[M+H]^+$; calcd. For $C_{30}H_{53}N_3O_7P$: 598,3621

Compound 13. Yield: 115mg (65%); as a white amorphous solid. A mixture of rotamers was observed by NMR (ratio 6:4). Assigned signals belong to the mixture of rotamers where (*) correspond to the major rotamer. R_f = 0.45 (hexane/EtOAc 1:1 v/v). ^{1}H NMR (400 MHz, $CDCl_3$) δ 8.23, 7.66* (2×s, 1H, NH), 7.44 – 7.15 (m, 5H), 5.16 (d, J = 15.8 Hz, 1H), 4.83 (d, J = 16.4 Hz, 1H), 4.53 – 4.41 (m, 2H), 4.28 – 4.04 (m, 4H), 3.65 – 3.57 (m, 1H), 3.42 (m, 4H), 2.24 – 2.11 (m, 1H), 2.08 – 1.82 (m, 4H), 1.81 – 1.67 (m, 2H), 1.46 (s, 9H), 1.33 (2×t, J = 7.1 Hz, 6H). ^{13}C NMR (100 MHz, $CDCl_3$) δ 174.66*, 173.13, 168.50*, 168.06, 155.15, 136.61, 129.19, 128.85, 128.60, 128.03, 127.84, 126.53, 80.43, 62.66*, 62.60, 62.34, 56.29, 55.66, 52.66*, 51.02, 50.67, 49.84, 47.29*, 47.19, 35.73, 34.17, 30.22*, 29.79, 28.63*, 28.54, 25.00, 16.59. HRMS (ESI–FT–ICR) m/z: 356,1376 $[M+H]^+$; calcd. for $C_{15}H_{23}N_3O_5P$: 356,1375

Compound 14. Yield: 161 mg (60%); as a white amorphous solid. R_f = 0.51 (hexane/EtOAc 1:1 v/v). ^{1}H NMR (400 MHz, $CDCl_3$) δ 7.55 – 7.25 (m, 5H), 6.63 (d, J = 2.7 Hz, 1H), 5.01 (d, J = 18.6 Hz, 1H), 4.71 (t, J = 15.2 Hz, 1H), 4.44 – 4.29 (m, 1H), 4.20 – 4.00 (m, 4H), 3.61 – 3.46 (m, 1H), 3.41 – 3.33 (m, 1H), 3.21 (ddd, J = 13.0, 8.6, 4.0 Hz, 1H), 2.27 – 2.08 (m, 1H), 2.02 (ddd, J = 20.0, 13.2, 7.0 Hz, 1H), 1.95 – 1.81 (m, 2H), 1.81 – 1.68 (m, 1H), 1.54 (s, 3H), 1.46 (s, 7H), 1.34 (t, J = 6.9 Hz, 3H), 1.28 (dd, J = 12.1, 5.0 Hz, 3H). ^{13}C NMR (101 MHz, $CDCl_3$) δ 175.03, 174.68, 154.92, 139.00, 129.06, 128.97, 127.59, 127.45, 126.39, 126.15, 80.12, 63.37, 62.69, 62.43, 62.38, 62.24, 62.17, 57.32, 48.11, 47.42, 35.55, 33.99, 31.71, 30.51, 28.75, 28.62, 25.30, 24.75, 23.57, 16.62, 16.56, 16.50, 16.44. HRMS (ESI–FT–ICR) m/z: 540,2833 $[M+H]^+$; calcd. for $C_{26}H_{43}N_3O_7P$: 540, 2839

Compound 15. Yield: 139 mg (45%); as a white amorphous solid. R_f = 0.30 (hexane/EtOAc 1:1 v/v). ^{1}H NMR (400 MHz, $CDCl_3$) δ 7.81 (d, J = 23.7 Hz, 3H), 7.55 (dd, J = 18.0, 7.5 Hz, 7H), 7.44 (t, J = 9.2 Hz, 5H), 7.38 – 7.19 (m, 44H), 5.66 – 5.41 (m, 7H), 4.96 (t, J = 15.1 Hz, 3H), 4.75 – 4.51 (m, 7H), 4.22 – 4.05 (m, 17H), 4.00 – 3.85 (m, 10H), 3.85 – 3.61 (m, 13H), 1.45 – 1.21 (m, 73H), 1.09 (qd, J = 7.0, 4.3 Hz, 16H).^{13}C NMR (100 MHz, $CDCl_3$) δ 168.86, 168.55, 156.19, 135.86, 134.94, 129.25, 129.16, 128.80, 128.69, 128.29, 127.11, 127.00, 80.33, 63.56, 53.11, 52.90, 51.19, 49.64, 46.49, 43.18, 28.50, 17.97, 16.58, 16.24. HRMS (ESI–FT–ICR) m/z: 619,1825 $[M+H]^+$; calcd. for $C_{30}H_{44}N_4O_8P$: 618,2819

Compound 16. Yield: 90 mg (40%); as a light yellow amorphous solid. R_f = 0.25 (hexane/EtOAc 1:3 v/v). ^{1}H NMR (400 MHz, $CDCl_3$) δ 7.22 – 7.05 (m, 5H), 6.99 (d, *J* = 7.1 Hz, 2H), 6.62 (d, *J* = 8.3 Hz, 2H), 6.41 (s, 1H), 5.81 (s, 1H), 4.67 (d, *J* = 17.6 Hz, 1H), 4.49 (d, *J* = 17.5 Hz, 1H), 4.16 – 3.99 (m, 4H), 3.90 – 3.73 (m, 1H),

3.61 (m, 1H), 2.06 (s, 3H), 1.32 – 1.23 (m, 6H). ^{13}C NMR (100 MHz, $CDCl_3$) δ 172.92, 170.48, 157.54, 137.41, 131.31, 128.58, 127.15, 126.26, 125.04, 115.93, 63.06, 50.85, 35.72, 34.15, 22.55, 16.48, 16.43, 14.31.

Compound 17. Yield: 97 mg (42%); as a colourless oil. R_f = 0.25 (hexane/EtOAc 1:3 v/v). ^{1}H NMR (400 MHz, $CDCl_3$) δ 7.22 – 7.05 (m, 5H), 6.99 (d, *J* = 7.1 Hz, 2H), 6.62 (d, *J* = 8.3 Hz, 2H), 6.41 (s, 1H), 5.81 (s, 1H), 4.67 (d, *J* = 17.6 Hz, 1H), 4.49 (d, *J* = 17.5 Hz, 1H), 4.16 – 3.99 (m, 4H), 3.90 – 3.73 (m, 1H), 3.61 (m, 1H), 2.06 (s, 3H), 1.32 – 1.23 (m, 6H). ^{13}C NMR (100 MHz, $CDCl_3$) δ 172.92, 170.48, 157.54, 137.41, 131.31, 128.58, 127.15, 126.26, 125.04, 115.93, 63.06, 50.85, 35.72, 34.15, 22.55, 16.48, 16.43, 14.31.

Computational methods

The conformational landscape of *cis–trans* isomers of *N*–alkylated peptides was explored in the gas phase by using the OPLS–2005 force–field [18] and a GB/SA chloroform solvent model, [19] as implemented in Macromodel version 9.9. [20] A 1000 steps Monte Carlo multiple minimum (MCMM) [23] and "Low–Mode" search algorithms [24] were combined to sample the conformational space of investigated peptoids, recording structure coordinates through an energy window of 5.0 kcal/mol relative to the lowest–energy conformation. It was carried out the clustering of conformers based on the distance between heavy atoms by using the Maestro program in version 5.7. [25] A maximum atom deviation of 0.5 Å was applied, including both heavy and hydrogen atoms to generate the root–mean–square matrix. The best cluster number was calculated through the average method for each case. A quantum mechanics (QM) energy minimization was carried out on each representative and clustered low–energy structure. Gaussian program in version 09 was used to perform the QM calculations using the M06–2X functional in combination with the 6–31G(d) basis set. [26] The pathway between minima separated by the transition state (TS) of the compounds (*S*)-3 and 9 was characterized by internal reaction coordinate (IRC) calculations. It was ensured the identification of the stationary points corresponding to minima or transition states on the potential energy hypersurface of 9. Subsequently, we choose a higher theory level (i.e. M06–2X/6–31+G(d,p)) to refine the electronic energies through further QM singlet–point calculations. In all QM calculations, the solvation contribution was included with the polarizable continuum solvation model SMD using chloroform as the solvent. Thus, the relative Gibbs free energies and Boltzmann populations at 25 °C were calculated from zero–point vibrational energy, entropic and thermal correction as described for each low–energy conformer quantically reoptimized in chloroform. The Cartesian coordinates are available in the Supporting Information, Part B, for all QM–optimized structures. Finally, a Natural Bond Orbital (NBO) analysis was performed at the M06–2X/6–31+G(d,p) level by using the NBO package [27] in version 5.0 as implemented in Gaussian 09 program. Both the Maestro suite [25] in version 5.7 and GaussView package [27] in version 5.0 were used for visualizing and drawing molecular structures.

Conclusions

In conclusion, we performed an NMR study and MCMM/QM calculations which reveal a different behaviour on the *cis–trans* isomerization of *N*–alkylated peptides synthesized by Ugi–4CR. We detected, that, when the POEG was introduced in the side chain of *N*–alkylated peptides, the three–dimensional structure preferentially adopts a *cis* conformation as occurring in 3. However, when the POEG was introduced in the backbone (i.e. compound 9), a mixture of *cis/trans* ratio was observed. Thus, these experimental findings are in full agreement with the quantum mechanics results, which allow rationalizing the *trans* and *cis* isomer preferences for the compounds 9 and 3, respectively. Finally, we introduced different oxo components in the Ugi–4CR. The NMR spectra exhibit only a *trans* isomer for the compounds 16 and 17, which was attributed to the $n\rightarrow\pi^*_{Ar}$ interaction.

Conflicts of interest

The authors declare no conflicts of interest.

Acknowledgements

This work was founded by the CONICYT FONDECYT 3170003. A. F. de la Torre is grateful to FONDECYT project No. 3170003 for financial support. We also thanks to VRID technician K. Bustamante for NMR measurements at the University of Concepcion. Akbar Ali is thankful to the TWAS–CNPq and HEC Pakistan (Project no. 21–2037/SRGP/R&D/HEC/2018). A.L.M.A is thankful to CONICYT/FONDECYT Iniciación 11180984 grant and Núcleo Milenio MULTIMAT, Chile. Powered@NLHPC: This research was partially supported by the supercomputing infrastructure of the NLHPC (ECM-02). E.W.H.R. and J.C. are thankful to CONICYT FONDECYT /INACH / POSTDOCTORADO/ Nº 3170107. We also thank the computing resources provided by the Department of Applied Physical Chemistry at the Universidad Autónoma de Madrid.

Notes and references

1 J. G. Allen, F. R. Atherton, M. J. Hall, C. H. Hassall, S. W. Holmes, R. W. Lambert, l. J. Nisbet and P. S. Ringrose, Nature, 1978, **272**, 56–58.

2 P. Kafarski and B. Lejczak, The biological activity of phosphono– and phosphinopeptides. In Aminophosphonic and Aminophosphinic Acids: Chemistry and Biological Activity, Kukhar VP, Hudson HR (eds.). John Wiley: Chichester, 2000, Chapter 12; 407–442.

3 a) FR. Atherton, CH. Hassall and RW. Lambert, J. Med. Chem. 1986, **29**, 29–40. b) S. Vassiliou, A. Grabowiecka, P. Kosikowska, A. Yiotakis, P. Kafarski and L. Berlicki, J. Med. Chem., 2008, **51**, 5736–5744. c) C. M. Armstrong, D. J. Meyers, L. S. Imlay, C. F. Meyers and A. R. Odom, Antimicrob. Agents Chemother., 2015, **59**, 5511–5519. d) B. S. Evans, C. Zhao, J. Gao, C. M. Evans, K. S. Ju, J. R. Doroghazi, W. A. Van Der Donk, N. L. Kelleher and W. W. Metcalf, ACS Chem. Biol., 2013, 8, 908–913. e) P. Kafarski and B. Lejczak, Phosphorus, Sulfur, and Silicon, 1991, **63**, 193–215. f) F. R. Atherton, M. J.

Hall, C. H. Hassall, R. W. Lambert and P. S. Ringrose, Antimicrob. Agents Chemother., 1979, **15**, 677–683. g) F. R. Atherton, M. J. Hall, C. H. Hassall and S. W. Holmes, 1980, **18**, 897–905. h) F. R. Atherton, C. H. Hassall and R. W. Lambert, J Med Chem, 1986, **29**, 29–40.

4 a) EL. Ravaschino, R. Docampo and JB. Rodriguez, J. Med. Chem. 2006, **49**, 426–435. b) E. Cunningham, M. Drag, P. Kafarski and A. Bell, Antimicrob. Agent Chemotherapy., 2008, **52**, 3221–3228.

5 E. De Clercq and A. Holý, Nat. Rev. Drug Discov., 2005, **4**, 928–940.

6 C. Adam, A. D. Peters, M. G. Lizio, G. F. S. Whitehead, V. Diemer, J. A. Cooper, S. L. Cockroft, J. Clayden and Simon J. Webb, Chem. Eur. J. 2018, **24**, 2249–2256.

7 I. M. Mándity and F. Fülöp, Expert Opin. Drug Discov. 2015, **10**, 1163–1177.

8 A. Trabocchi and A. Guarna. Peptidomimetics in Organic and Medicinal Chemistry: The Art of Transforming Peptides in Drugs, First Edition. © 2014 John Wiley & Sons, Ltd. Published 2014 by John Wiley & Sons, Ltd. Chapter 6, pp. 121–135.

9 For reviews on peptoids see: a) I. Mándity and F. Fülöp, Expert Opinion on Drug Discovery., 2015, **10** (11), 1163–1177. b) R.N. Zuckermann, Pept. Sci., 2011, **96** (5), 545–555. b) C.A. Olsen, ChemBioChem, 2010, **11**, 152. c) B. Yoo, and K. Kirshenbaum, Curr. Opin. Chem. Biol., 2008, **12**, 714. d) S.A. Fowler, and H.E. Blackwell, Org. Biomol. Chem., 2009, **7**, 1508. e) R.N. Zuckermann, and T. Kodadek, Curr. Opin. Mol. Ther., 2009, 11, 299. f) N. Gangloff, J. Ulbricht, T. Lorson, H. Schlaad, and R. Luxenhofer, Chemical Reviews., 2016, **116** (4), 1753–1802.

10 For solid phase peptoids synthesis see: a) T. S. Burkoth, A. T. Fafarman, D. H. Charych, M. D. Connolly and R. N. Zuckermann, J. Am. Chem. Soc., 2003, **125**, 8841. b) H. Jang, A. Fafarman, J.M. Holub and K. Kirshenbaum, Org. Lett., 2005, **7**, 1951. c) R.N. Zuckermann, J.M. Kerr, S.B.H. Kent and W.H. Moos, J. Am. Chem. Soc., 1992, **114**, 10646–10647.

11 For cis–trans studies see: a) B. C. Gorske, B. L. Bastian, G. D. Geske and H. E. Blackwell, J. Am. Chem. Soc., 2007, **129** (29), 8928–8929. b) J. S. Laursen, J. E. Andreasen, P. Fristrup, P. Harris, and C. A. Olsen. J. Am. Chem. Soc., 2013, **135** (7), 2835–2844. c) B. C. Gorske, J. R. Stringer, B. L. Bastian, S. A. Fowler and H. E. Blackwell, Journal of the American Chemical Society. 2009, **131** (45), 16555–16567. d) J. Engel–Andreasen, K. Wich, J.S. Laursen, P. Harris, and C. A. Olsen. The Journal of Organic Chemistry. 2015, **80** (11), 5415–5427.e) J. R. Stringer, J. A. Crapster, I. A. Guzei, and H. E. Blackwell, The Journal of Organic Chemistry 2010 75 (18), 6068–6078. f) G. L. Butterfoss, P. D. Renfrew, B. Kuhlman, K. Kirshenbaum and R. Bonneau. Journal of the American Chemical Society., 2009, **131** (46), 16798–16807. g) M. M. Zimnicka. The Journal of Physical Chemistry A.; 2018, **122** (39), 7819–7831. h) G. Dumonteil, N. Bhattacharjee, G. Angelici, O. Roy, S. F. Laurent, J. Franck, J. Lionel, P. Claude, T. fumier, The Journal of Organic Chemistry., 2018, **83** (12), 6382–6396.

12 For n→π* interaction see: a) R. W. Newberry and R. T. Raines, Accounts of Chemical Research., 2017, **50** (8), 1838–1846. b) S. K. Singh, K. K. Mishra, N. Sharma, A. Das. Angewandte Chemie International Edition. 2016, **55** (27), 7801–7805. c) R. W. Newberry and R. T. Raines, ACS Chemical Biology. 2014, **9** (4), 880–883. d) B. C. Gorske, R. C. Nelson, Z. S. Bowden, T. A. Kufe and A. M. Childs, The Journal of Organic Chemistry., 2013, **78** (22), 11172–11183. e) R. W. Newberry, B. VanVeller, I. A. Guzei and R. T. Raines, Journal of the American Chemical Society. 2013, **135** (21), 7843–7846. f) K. J. Kamer, A. Choudhary and R. T. Raines, The Journal of Organic Chemistry. 2013, **78** (5), 2099–2103

13 J. A. Crapster, J. R. Stringer, I.A. Guzei and H. E. Blackwell, Pept. Sci., 2011, **96**(5), 605–616.

14 A. F. de la Torre, D. G. Rivera, M. A. B. Ferreira, A. G. Corrêa, and M. W. Paixão, J. Org. Chem., 2013, **78** (20), 10221–10232.

15 For ugi synthesis of peptoids see: a) I. Ugi, R. Meyr, U. Fetzer, C. Steinbrücker, Angew. Chem. 1959, 71, 386. b) S. Marcaccini, and T. Torroba, Nature Protocols., 2007, 2, 632–639 b) F. E. Morales, H. E. Garay, D. F. Muñoz, Y. E. Augusto, A. J. Otero–González, O. Reyes Acosta and D. G. Rivera, Org. Lett., 2015, 17 (11), 2728–2731. c)M. L. Bode, D. Gravestock, A. L. Rousseau. Organic Preparations and Procedures International. 2016, 48 (2), 89–221. d) M. Hartweg, C. J. C. Edwards–Gayle, E. Radvar, D. Collis, M. Reza, M. Kaupp, J. Steinkoenig, J. Ruokolainen, R. Rambo, C. Barner–Kowollik, I. W. Hamley, H. S. Azevedo and C. R. Becer, Polym. Chem., 2018, 9, 482–489.

16 a) A. F. G. Gargano, S. Buchinger, M. Kohout, W. Lindner and M. Lämmerhofer, J. Org. Chem., 2013, **78**, 10077–87. b) S. Abás, C. Estarellas, F. Javier Luque and C. Escolano, Tetrahedron, 2015, **71**, 2872–2881.

17 I. Hoppe and U. Schiillkopf, Chem. Ber., ***109***: 482, 1976.

18 W. C. Still, A. Tempczyk, R. C. Hawley and T. Hendrickson, J. Am. Chem. Soc., 1990, **112**, 6127−6129.

19 G. A. Kaminski, R. A. Friesner, J. Tirado–Rives, W. Jorgensen, J. J. Phys. Chem. B., 2001, **105**, 6474−6487.

20 a) MacroModel, v. 9.9; Schrödinger Inc.: Cambridge, MA, 2012; http://www.schrodinger.com. b) F. Mohamadi, N. G. J. Richards, W. C. Guida, R. Liskamp, M. Lipton, C. Caulfield, G. Chang, T. Hendrickson and W. C. J. Still, Comput. Chem., 1990, **11**, 440−467.

21 R. N. V. K. Deepak, and R. Sankararamakrishnan, Biochemistry, 2016, **55**, 3774-3783.

22 R. K. Deepak, and R. Sankararamakrishnan, Biophys. J., 2016, **110**, 1967-1979.

23 G. Chang, W. C. Guida, W. C. Still, J. Am. Chem. Soc., 1989, **111**, 4379−4386.

24 M. Saunders, K. N. Houk, Y.–D. Wu, W. Still, C. M. Lipton, G. Chang, W. C. Guida, J. Am. Chem. Soc. 1990, **112**, 1419−1427.

25 "Maestro, version 9.3, Schrödinger, LLC, New York, NY, 2012. Schrödinger, L. Desmond Molecular Dynamics System, Version 3.0; Epik Version 2.2; Glide, Version 5.7; Impact, Version 5.7; LigPrep, Version 2.5; Phase, Version 3.3; Prime, Version 2.3; SiteMap, Version 2.5; Virtual Screening Workflow. *New York, NY* **2011**."
Falta revisar estas referencias

26 M.J. Frisch, Gaussian 09, Revision A.02; Gaussian, Inc.: Wallingford, CT. (2009).

27 a) NBO 5.0. E. D. Glendening, J. K. Badenhoop, A. E. Reed, J. E. Carpenter, J. A. Bohmann, C. M. Morales, and F. Weinhold (Theoretical Chemistry Institute, University of Wisconsin, Madison, WI, 2001). b) M.J. Frisch, G.W. Trucks, H.B. Schlegel, M.J. Frisch, G.W. Trucks, H.B. Schlegel, G.E. Scuseria, M.A. Robb, J.R. Cheeseman, G. Scalmani, V. Barone, B. Mennucci, G.A. Petersson, Gaussian 09, Revision A.02, (2009). https://www.scienceopen.com/document?vid=6be7271f–f651–464b–aee6–ef20b0743b6b (accessed October 24, 2018).

View Article Online
DOI: 10.1039/C9NJ02234A

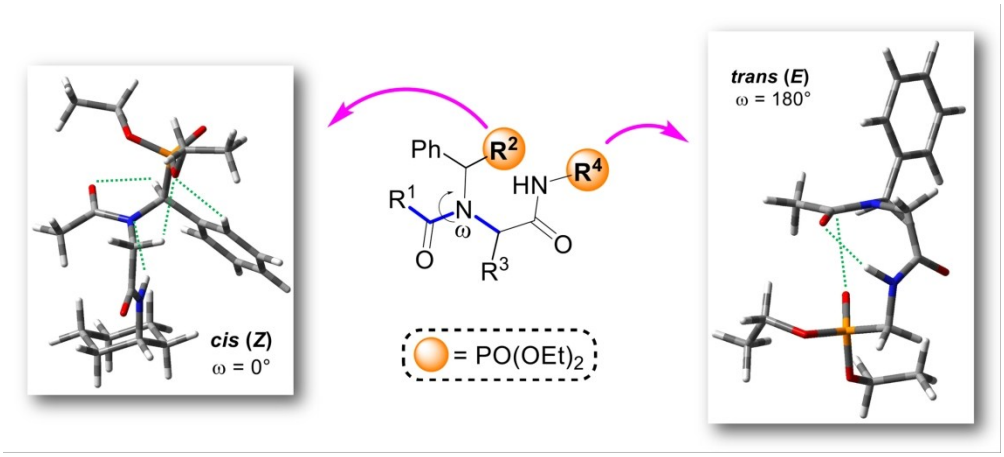

100x45mm (600 x 600 DPI)